and development of low-noise microwave tubes. In 1958, he became Assistant Professor of Physics at Union College, Schenectady, NY. In 1960, he joined RCA Laboratories as a member of technical staff. There he engaged in research on microwave power tubes, multivelocity flow problems in electron beams and plasmas, and microwave solid-state devices. He has been directing projects in microwave integrated circuits since 1966, and has authored numerous papers in this field. He has worked on the basic design and measurement of microstrip circuits and integration methods based on the use of lumped elements for the miniaturization of high-power amplifiers and microwave circuits, including FET devices. He has coauthored a textbook, *Physical Electronics* (John Wiley & Sons, Inc., NY 1967), and has also taught courses in microwaves and modern physics as Adjunct Professor of Electrical Engineering at Drexel Institute of Technology. During 1971–1972, he served as Visiting Professor at the Technion (Israel Institute of Technology) in Haifa, Israel.

Dr. Caulton was the recipient of RCA Laboratories' Achievement Awards for his work in microwave integrated circuits in 1968 and 1971. From 1970 to 1975, he served first as Cochairman and later as Chairman of the Committee on Microwave Integrated Circuits of IEEE Microwave Theory and Techniques Society and was formerly an Associate Editor of IEEE TRANSACTIONS OF MICROWAVE THEORY AND TECHNIQUES. He is a member of the American Physical Society and Sigma Xi.

✤

Arye Rosen (M'77–SM'80) received the B.S.E.E. degree cum laude from Howard University in 1963 and the M.Sc.E. degree from Johns Hopkins University, Baltimore, MD, which he attended on a Gillman Fellowship, in 1965. He received the M.Sc. degree in physiology at Jefferson Medical College, Philadelphia, PA.

During the years 1963–1964, he was an instructor at John Hopkins. From 1964 to 1967, he was concerned with systems design at General Telephone and Electronics International, and with antenna and circuit design at Channel Master, Inc., and American Electronics Laboratories, Inc. In 1967, Mr. Rosen joined RCA Laboratories, where is is presently engaged in the study of development of microwave circuits and devices. From 1970 to 1971, on leave of absence from RCA, he was engaged in research in the Division of Cardiology at Jefferson Medical College in Philadelphia, PA, where he presently holds an appointment as an Associate in Medicine. He is the author of over 35 technical papers and presentations and holds 20 patents in the microwave field; he is also the author of several papers and presentations in the field of echocardiography.

Mr. Rosen is the recipient of a 1972 RCA Laboratories Outstanding Achievement Award for a team effort in the development of *S*-band TRAPATT amplifiers. He is a member of Tau Beta Pi, Sigma Xi, and the Association of Professional Engineers of British Columbia.

✤

Paul Stabile (S'75–M'79) received the B.E. degree in electrical engineering summa cum laude from Manhattan College, Bronx, NY, in 1979.

Afterward, he entered the Engineering Rotation Program at RCA. His assignments included microwave amplifier design, digital circuit development, and a study of VLSI computer-aided design techniques. In October 1979, he joined RCA Laboratories, where is is presently an Associate Member of technical staff. There he has been engaged in research of high power, low-frequency p-i-n diodes, and silicon millimeter-wave devices and integrated circuits. He is also the author of several technical papers.

Mr. Stabile is a member of Eta Kappa Nu, Tau Beta Pi, and Epsilon Sigma Pi of Manhattan College.

✤

Anna M. Gombar was born in Hungary. After attending the Technical University in Budapest, she came to the United States in 1956.

In 1960, she began textile research at F.M.C. in Princeton, NJ. Transfering to RCA Laboratories in 1973, she was engaged in research in the field of silicon devices such as high-power p-i-n diodes, high Q varacter diodes, and lately, millimeter-wave device technology. She is the holder of several U.S. patents and the author of several technical publications.

Coupling Characteristics Between Single-Mode Fiber and Square Law Medium

RYOZO KISHIMOTO, MEMBER, IEEE, AND MASAKI KOYAMA, MEMBER, IEEE

Abstract — **The coupling characteristics between a single-mode fiber and a square law medium are theoretically and experimentally discussed in order to obtain the optimum coupling design for a variety of single-mode fiber optical devices using square law media. In theoretically analyzing coupling efficiency, it has been possible to evaluate a Gaussian beam, in a dielectric, which has passed through a square law medium with the help of mode-expansion technique and one of the generating functions of the Hermite polynomials. As a result, it has been possible to analytically obtain coupling efficiency even when the output beam from the single-mode fiber is off-axis and tilted. Through this analysis, it has been made clear that the ray matrix analysis used previously agrees with the analysis without the**

Manuscript received October 8, 1981; revised December 30, 1981.

The authors are with the Electrical Communication Laboratories, Nippon Telegraph and Telephone Public Corporation, 1-2356, Take, Yokosuka-shi, Kanagawa-Ken, 238-03, Japan.

0018-9480/82/0600-0882$00.75 ©1982 IEEE

off-axis and tilt factors analyzed in this paper. The experimental results concerning the optimum coupling design, the off-axis characteristics, and the off-axis tolerances have been presented and agree well with the theoretical analysis.

I. Introduction

OPTICAL transmission systems using laser diodes and single-mode silica optical fibers are valuable as optical transmission systems with large capacity and long repeater spacing for low-loss and low-dispersion characteristics. Especially in the 1–1.8-μm wavelength region, a zero dispersion wavelength exists where the wavelength dispersion for single-mode fiber disappears. Because of the wide-band characteristics at wavelengths close to the zero dispersion wavelength, the repeater spacing is restricted mainly by the fiber loss and coupling loss of optical devices, such as the laser module and optical connector. Reductions in fiber loss and coupling loss are significant ways of extending the repeater spacing. Therefore, in order to realize the above system, not only is the reduction in fiber loss important. Equally critical is the reduction in coupling loss for optical devices inserted in the optical transmission line.

Many optical device construction methods have been proposed [1]. In one such method, microoptic devices have been employed using a square law medium in many cases [2], [3], in order that they may be small, have low loss and be easy to produce. In considering optimum optical device construction, it is necessary to accurately understand the off-axis and tilt characteristics for coupling efficiency, such as those between fiber and square law medium. However, until now only experimental investigations in many reports [4] have been accomplished and no theoretical investigation has been reported.

On the other hand, many analyses of square law media have been reported [5], [6], [7]. However, no analysis of a Gaussian beam passed through a square law medium of an incident beam with off-axis and tilt factors has yet been reported. But there has been Gaussian beam analysis [8] of an incident beam with only the off-axis calculated, using the input-beam mode-expansion technique and the Fresnel–Kirchhoff integral. In the above analysis, the coupling efficiency calculation seems to be very complex, as the Gaussian beam which has passed through the square law medium is expressed as a summation.

The purpose of this paper is to theoretically and experimentally make clear the coupling characteristics between a single-mode fiber and a square law medium when the output beam from a single-mode fiber which is off-axis and tilted is incident at another single-mode fiber through two square law media. In analyzing theoretically the coupling efficiency between a single-mode fiber and a square law medium, the Gaussian beam in the square law medium excited by the output beam from a single-mode fiber is at first expanded in an infinite series with the help of the modes of the square law medium. Next, the Gaussian beam in the dielectric passed through the square law medium is expanded in an infinite series with the help of the modes of the dielectric. These infinite series can be evaluated with the help of one of the generating functions of the Hermite polynomials. Therefore, the coupling efficiency can be analytically obtained even when the output beam from a single-mode fiber is off-axis and tilted. As the result of this analysis, it is made clear that the ray matrix analysis used previously agrees with the analysis without the off-axis and tilt factors analyzed in this paper. Finally, experimental coupling results which agree well with the above theoretical analysis are presented.

II. Gaussian Beam in Square Law Medium

As shown in Fig. 1, a square law medium is placed between dielectric #1 and dielectric #2. The optical axis is equal to the z-axis. The refractive index of the square law medium is expressed by

$$n_{sq}(x, y) = n_s\{1 - g^2 \cdot (x^2 + y^2)\}^{1/2} \qquad (-l_1 \leqslant z \leqslant 0) \tag{1}$$

where n_s is the refractive index of the square law medium on the optical axis. The square law medium modes are Hermite–Gaussian functions. The general mode solution of the square law medium is

$$\psi_{pq}^{(1)}(x, y, z) = \phi_{pq}^{(1)}(x, y)\exp\left(-j\gamma_{pq}^{(1)}z\right) \qquad (-l_1 \leqslant z \leqslant 0) \tag{2}$$

$$\phi_{pq}^{(1)}(x, y) = \frac{\sqrt{2}/w_1}{\sqrt{\pi 2^{p+q} p!q!}} H_p\left(\frac{\sqrt{2}}{w_1}x\right) H_q\left(\frac{\sqrt{2}}{w_1}y\right) \cdot \exp\{-(x^2 - y^2)/w_1^2\} \tag{3}$$

and

$$\gamma_{pq}^{(1)} = n_s k_0 - (p + q + 1)g$$
$$w_1 = (2/n_s k_0 g)^{1/2}$$
$$k_0 = 2\pi/\lambda_0 \tag{4}$$

where g is the focusing parameter of the square law medium, w_1 is the radius of the eigenspot size in the square law medium, and λ_0 is a wavelength in free space. $H_p(x)$ represents pth-order Hermite polynomials and is given by

$$H_p(x) = (-1)^p e^{x^2} \frac{d^p}{dx^p} e^{-x^2}. \tag{5}$$

The authors assume that the refractive index values in dielectrics #1 and #2 are n_1 and n_2, respectively.

The transmitted field in the square law medium is considered for a Gaussian beam $\Phi(x, y, z)$ radiated from a single-mode fiber incident from dielectric #1 on a boundary plane ($z = -l_1$) of the square law medium. The fiber axis is tilted by θ rad on the $x-z$ plane and is displaced by h_x on the $x-z$ plane and by h_y on the $y-z$ plane from the axis of the square law medium. The reflected field at $z = -l_1$ is ignored. The Gaussian beam, which is incident on a point $(h_x, h_y, -l_1)$ of the boundary plane $z = -l_1$ with the smallest spot size w_s at $z = -z_s$ and a direction cosine

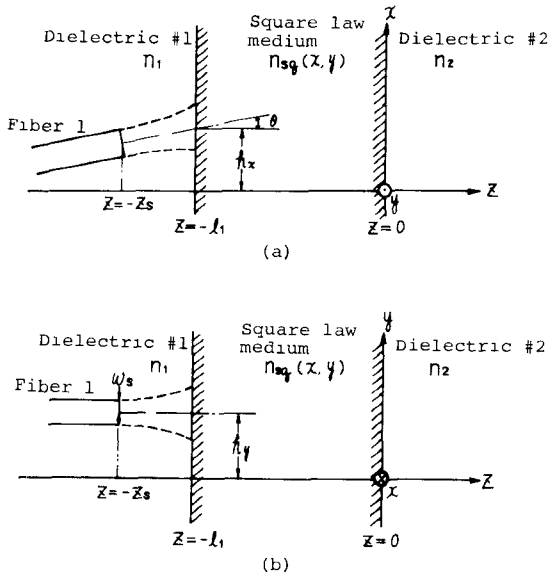

Fig. 1. Configuration of a square law medium and a single-mode fiber (a) $x-z$ plane (b) $y-z$ plane.

$(\theta, 0, 1-\theta^2/2)$ is given by

$$\Phi(x,y,z)=\frac{\sqrt{2}}{\sqrt{\pi}\,w}\exp\left[-\left(\frac{1}{w^2}+j\frac{n_1k_0}{2R}\right)\cdot\left\{(x-h_x-l_1\theta-z\theta)^2+(y-h_y)^2\right\}\right.$$

$$-jn_1k_0\left\{\theta(x-h_x-l_1\theta)+(1-\theta^2/2)z+(1+\theta^2/2)z_s\right\}$$

$$\left.+j\tan^{-1}\left\{\frac{2(z+z_s)}{n_1k_0w_s^2}\right\}\right]\qquad(z\leqslant -l_1)\tag{6}$$

and

$$w=w_s\left[1+\left\{2(z+z_s)/n_1k_0w_s^2\right\}^2\right]^{1/2}$$
$$R=(z+z_s)\left[1+\left\{n_1k_0w_s^2/2(z+z_s)\right\}^2\right]\tag{7}$$

where w and R are the spot size radius and the radius of curvature of the wavefront for the incident Gaussian beam, respectively [9].

The transmitted field F^t in the square law medium can be expanded in an infinite series with the help of the modes of the square law medium given by (2)

$$F^t(x,y,z)=\sum_{p,q}C_{pq}\psi_{pq}(x,y,z)\qquad(-l_1\leqslant z\leqslant 0).\tag{8}$$

The expansion coefficients C_{pq} have been determined at $z=-l_1$, with the reflected field at $z=-l_1$ being ignored. Using the orthogonality of the modes, we obtain

$$C_{pq}=\exp\left(-j\gamma_{pq}^{(1)}l_1\right)\iint_{-\infty}^{\infty}\Phi(x,y,-l_1)\phi_{pq}^{(1)}(x,y)\,dx\,dy.\tag{9}$$

The integral in (9) can be solved with the help of the integral tables of Gradshteyn and Ryzhik, with the result that

$$C_{pq}=\frac{W_g\zeta^{(p+q)/2}}{\sqrt{2^{(p+q)}p!q!}}H_p(\rho_x)H_q(\rho_y)\exp\left(-j\gamma_{pq}^1l_1\right)\tag{10}$$

and

$$W_g=2\frac{w_1}{w_{l1}}\left(1+\frac{w_1^2}{w_{l1}^2}+j\frac{w_1^2n_1k_0}{2R_{l1}}\right)^{-1}\cdot\exp\left[jn_1k_0\left\{\theta h_x+(1+\theta^2/2)(l_1-z_s)\right\}\right.$$

$$+j\tan^{-1}\left\{\frac{2(z_s-l_1)}{n_1k_0w_s^2}\right\}-\left(1+\frac{w_1^2}{w_{l1}^2}+j\frac{w_1^2n_1k_0}{2R_{l1}}\right)^{-1}\cdot\left\{\left(\frac{w_1n_1k_0\theta}{2}\right)^2+j(w_1n_1k_0\theta)\cdot\frac{h_x}{w_1}\left(\frac{w_1^2}{w_{l1}^2}+j\frac{w_1^2n_1k_0}{2R_{l1}}\right)\right.$$

$$\left.\left.+\left(\frac{w_1^2}{w_{l1}^2}+j\frac{w_1^2n_1k_0}{2R_{l1}}\right)\left(\frac{h_x^2}{w_1^2}+\frac{h_y^2}{w_1^2}\right)\right\}\right]$$

$$\zeta=\left(-1+\frac{w_1^2}{w_{l1}^2}+j\frac{w_1^2n_1k_0}{2R_{l1}}\right)\cdot\left(1+\frac{w_1^2}{w_{l1}^2}+j\frac{w_1^2n_1k_0}{2R_{l1}}\right)^{-1}$$

$$\rho_x=\sqrt{2}\left\{\left(\frac{w_1^2}{w_{l1}^2}+j\frac{w_1^2n_1k_0}{2R_{l1}}\right)\frac{h_x}{w_1}-j\frac{w_1n_1k_0\theta}{2}\right\}\cdot\left[\left(-1+\frac{w_1^2}{w_{l1}^2}+j\frac{w_1^2n_1k_0}{2R_{l1}}\right)\left(1+\frac{w_1^2}{w_{l1}^2}+j\frac{w_1^2n_1k_0}{2R_{l1}}\right)\right]^{-1/2}$$

$$\rho_y=\sqrt{2}\left\{\left(\frac{w_1^2}{w_{l1}^2}+j\frac{w_1^2n_1k_0}{2R_{l1}}\right)\frac{h_y}{w_1}\right\}\left[\left(-1+\frac{w_1^2}{w_{l1}^2}+j\frac{w_1^2n_1k_0}{2R_{l1}}\right)\cdot\left(1+\frac{w_1^2}{w_{l1}^2}+j\frac{w_1^2n_1k_0}{2R_{l1}}\right)\right]^{-1/2}\tag{11}$$

where w_{l1} and R_{l1} are w and R at $z=-l_1$, respectively. The field distribution at any arbitrary point in the square law medium can be expressed from (8) and (10) by the equation

$$F^t(x,y,z)=\sqrt{\frac{2}{\pi}}\frac{W_g}{w_1}\exp\left\{-j(n_sk_0-g)(l_1+z)\right\}\cdot\exp\left\{-(x^2+y^2)/w_1^2\right\}\cdot\sum_{p,q}\frac{1}{p!q!}\left(\frac{\sqrt{\zeta}\exp\left\{jg(l_1+z)\right\}}{2}\right)^{p+q}\cdot H_p(\rho_x)H_q(\rho_y)H_p\left(\frac{\sqrt{2}}{w_1}x\right)H_q\left(\frac{\sqrt{2}}{w_1}y\right).\tag{12}$$

The infinite series can be evaluated with the help of one of the generating functions of the Hermite polynomials given by

$$\sum_{p=0}^{\infty} \frac{1}{p!}\left(\frac{Z}{2}\right)^p H_p(X)H_p(Y) = (1-Z^2)^{-1/2}\exp\left[\frac{2XYZ-(X^2+Y^2)Z^2}{1-Z^2}\right]. \tag{13}$$

We thus obtain

$$F'(x,y,z) = \sqrt{\frac{2}{\pi}}\frac{W_g}{w_1}\exp\{-j(n_s k_0 - g)(l_1+z)\} \cdot\left(1-\zeta\exp\{2jg(l_1+z)\}\right)^{-1} \cdot\exp\left[-\frac{(x^2+y^2)(1+\zeta\exp\{2jg(l_1+z)\})}{w_1^2(1-\zeta\exp\{2jg(l_1+z)\})}\right] \cdot\exp\left[\frac{2\sqrt{\zeta}\exp\{jg(l_1+z)\}\frac{\sqrt{2}}{w_1}(\rho_x\cdot x+\rho_y\cdot y)}{1-\zeta\exp\{2jg(l_1+z)\}}\right] \cdot\exp\left[\frac{-(\rho_x^2+\rho_y^2)\zeta\exp\{2jg(l_1+z)\}}{1-\zeta\exp\{2jg(l_1+z)\}}\right].$$

Figs. 2 and 3 show examples of calculated results regarding field distribution in the square law medium. The parameters of the single-mode fiber used in the calculations are a 10-μm core diameter, 1.46 refractive index, and 0.24-percent relative refractive-index difference between the core and cladding. The g, n_s, and l_1 for the square law medium used in calculations are $\pi/10$ mm^{-1}, 1.58, and 10 mm, respectively. Radius w_s of the spot size of the single-mode fiber at $z=-z_s$ is given by [10]

$$w_s = a(0.65+1.619/V^{1.5}+2.879/V^6)$$
$$V = \frac{2\pi}{\lambda_0}n_0 a\sqrt{2\Delta} \tag{15}$$

where a is the core radius for a single-mode fiber, Δ is a relative refractive-index difference between the core and cladding, and V is the cutoff normalized frequency. Fig. 2 shows the field distribution $|F'|$ along the x-axis ($y=0$) in the square law medium, which has been normalized by $|F'|$ at $z=-9$ mm, when the radiated Gaussian beam from a single-mode fiber is incident at the boundary plane ($z=-l_1$) of the square law medium with the single-mode fiber being off-axis. The off-set parameter h_x along the x-axis is 400 μm, h_y along the y-axis is 0 μm, and the distance (z_s-l_1) between the single-mode fiber and the square law medium is 100 μm. The center axis of the field distribution $|F'|$ gradually brings the optical axis of the square law medium closer while transmitting in the z-direction. $|F'|$ is the Gaussian beam which is almost symmetrical with respect to the optical axis of the square law medium at $z=-5$ mm, and is expanding in the negative x-direction while propagating in the z-direction. Fig. 3 shows the field distribution $|F'|$ with an angle $\theta=-2°$ in addition to its condition in Fig. 2. $|F'|$ is already expanding in the negative x-direction at $z=-5$ mm (which corresponds to 1/4 pitch).

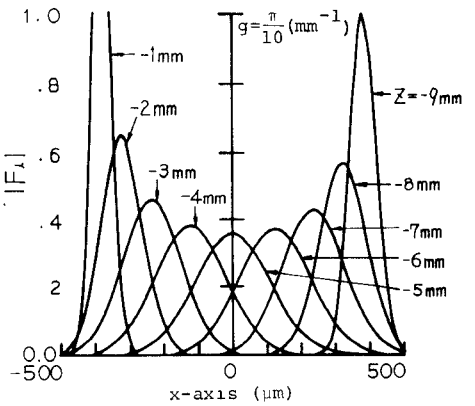

Fig. 2 Calculated results of the field distribution $|F'|$ along the x-axis ($y=0$) in the square law medium, normalized by $|F'|$ at $z=-9$ mm, when the radiated Gaussian beam from a single-mode fiber is incident at the boundary plane ($z=-l_1$) with a single-mode fiber being off axis ($h_x=400$ μm)

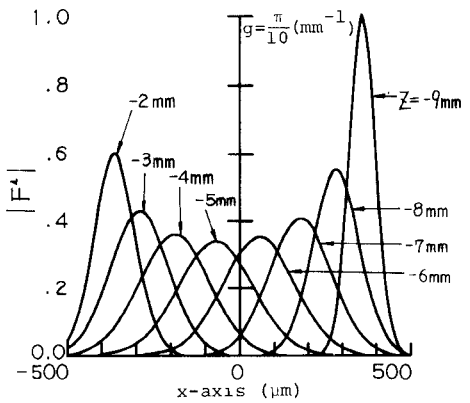

Fig. 3. Calculated results of the field distribution $|F'|$ with an angle $\theta=-2°$ in addition to the condition of $|F'|$ in Fig. 2.

III. Gaussian Beam Passed through Square Law Medium

Consider that the Gaussian beam F^i in the square law medium is radiated from the boundary plane ($z=0$) to dielectric #2. The reflected beam at $z=0$ is ignored. The Gaussian beam F^i excites the transmitted Gaussian beam F^t propagating in the positive z-direction in dielectric #2. It is assumed that the Hermite Gaussian function is an eigen function $\psi_{mn}^{(2)}(x,y,z)$ of dielectric #2. The transmitted Gaussian beam F^t in dielectric #2 can be expanded in an infinite series with the help of $\psi_{mn}^{(2)}(x,y,z)$.

The transmitted Gaussian beam F^t can be expressed by

$$F^t(x,y,z) = \sum_{m,n} t_{mn}\psi_{mn}^{(2)}(x,y,z) \qquad (z\geq 0). \tag{16}$$

The transmitted expansion coefficients t_{mn} are given by (17), using the orthogonality of the modes

$$t_{mn} = \int^{-\infty}\int_{\infty}\psi_{mn}^{(2)*}(x,y,0)\sum_{p,q}C_{pq}\phi_{pq}^{(1)}(x,y)\,dx\,dy. \tag{17}$$

The Hermite Gaussian function $\psi_{mn}^{(2)}$, which is the eigenfunction for dielectric #2, is given by

$$\psi_{mn}^{(2)}(x,y,z)=\frac{\sqrt{2}/w_t(z)}{\sqrt{\pi 2^{p+q}p!q!}}H_m\left(\frac{\sqrt{2}}{w_t(z)}x\right)H_n\left(\frac{\sqrt{2}}{w_t(z)}y\right)$$
$$\cdot\exp\left\{\frac{-(x^2+y^2)}{w_t(z)^2}\right\}\exp\left[-j\left\{\frac{n_2k_0(x^2+y^2)}{2R_t(z)}+n_2k_0z\right.\right.$$
$$\left.\left.\cdot-(m+n+1)\phi_t(z)\right\}\right] \tag{18}$$

and

$$w_t(z)=w_2\left[1+\left\{2(z-z_2)/n_2k_0w_2^2\right\}^2\right]^{1/2}$$
$$R_t(z)=(z-z_2)\left[1+\left\{n_2k_0w_2^2/2(z-z_2)\right\}^2\right]$$
$$\phi_t(z)=\tan^{-1}\left\{2(z-z_2)/n_2k_0w_2^2\right\} \tag{19}$$

where w_2 is the radius of the smallest spot size of $\psi_{mn}^{(2)}(x,y,z)$ and z_2 is the distance between the boundary plane ($z=0$) and the beam waist of $\psi_{mn}^{(2)}(x,y,z)$.

The transmitted expansion coefficients t_{mn} are given by

$$t_{mn}=2W_g\frac{w_t(0)}{w_1}\frac{1}{\sqrt{2^{m+n}m!n!}}(1-\zeta\exp(2jgl_1))^{-1}$$
$$\cdot(\zeta_1+j\zeta_2)^{-1}\left(\frac{\zeta_1-2+j\zeta_2}{\zeta_1+j\zeta_2}\right)^{(m+n)/2}$$
$$\cdot H_m\left[\frac{2\sqrt{\zeta}\,(w_t(0)/w_1)\rho_x\exp(jgl_1)}{1-\zeta\exp(2jgl_1)}\right.$$
$$\left.\cdot\{(\zeta_1+j\zeta_2)(\zeta_1-2+j\zeta_2)\}^{-1/2}\right]$$
$$\cdot H_n\left[\frac{2\sqrt{\zeta}\,(w_t(0)/w_1)\rho_y\exp(jgl_1)}{1-\zeta\exp(2jgl_1)}\right.$$
$$\left.\cdot\{(\zeta_1+j\zeta_2)(\zeta_1-2+j\zeta_2)\}^{-1/2}\right]$$
$$\cdot\exp\left[-\frac{\zeta\exp(2jgl_1)\left(\rho_x^2+\rho_y^2\right)}{1-\zeta\exp(2jgl_1)}\right.$$
$$\left.\cdot\left(1-\frac{2\left(w_t(0)^2/w_1^2\right)}{(\zeta_1+j\zeta_2)\{1-\zeta\exp(2jgl_1)\}}\right)\right]$$
$$\cdot\exp[-j\{(m+n+1)\phi_t(0)+(n_1k_0-g)l_1\}] \tag{20}$$

where

$$\zeta_1+j\zeta_2=1+w_t(0)^2/w_1^2-j\frac{w_t(0)^2n_2k_0}{2R_t(0)}$$
$$+\frac{2w_t(0)^2/w_1^2}{1-\zeta\exp(2jgl_1)}\cdot\zeta\exp(2jgl_1). \tag{21}$$

The transmitted Gaussian beam F^t can be expressed analytically with the help of the generating functions of the Hermite polynomials (13) by

$$F^t(x,y,z)=2\sqrt{\frac{2}{\pi}}\frac{W_g}{w_1}\frac{w_t(0)}{w_t(z)}$$
$$\cdot(1-\zeta\exp(2jgl_1))^{-1}(\zeta_1+j\zeta_2)^{-1}$$
$$\cdot\left(1-(\zeta_3+j\zeta_4)\exp\{2j(\phi_t(z)-\phi_t(0))\}\right)^{-1}$$
$$\cdot\exp\left\{-(x^2+y^2)/w_t(z)^2\right\}$$
$$\cdot\exp\left[-j\left\{\frac{n_2k_0(x^2+y^2)}{2R_t(z)}+n_2k_0z-\phi_t(z)\right.\right.$$
$$\left.\left.+\phi_t(0)+(n_sk_0-g)l_1\right\}\right]\exp\left[-\frac{\zeta\exp(2jgl_1)\left(\rho_x^2+\rho_y^2\right)}{1-\zeta\exp(2jgl_1)}\right.$$
$$\left.\cdot\left(1-\frac{2w_t(0)^2/w_1^2}{(\zeta_1-j\zeta_2)\{1-\zeta\exp(2jgl_1)\}}\right)\right]$$
$$\cdot\exp\left[\left[2\sqrt{\zeta_3+j\zeta_4}\cdot\exp\{j(\phi_t(z)-\phi_t(0))\}\frac{\sqrt{2}}{w_t(z)}\right.\right.$$
$$\cdot(\rho_{1x}\cdot x+\rho_{1y}\cdot y)-\left\{\rho_{1x}^2+\rho_{1y}^2+2(x^2+y^2)/w_t(z)^2\right\}$$
$$\left.\cdot(\zeta_3+j\zeta_4)\exp\{2j(\phi_t(z)-\phi_t(0))\}\right]$$
$$\left./\left[1-(\zeta_3+j\zeta_4)\exp\{2j(\phi_t(z)-\phi_t(0))\}\right]\right] \tag{22}$$

and

$$\zeta_3=\{\zeta_1(\zeta_1-2)+\zeta_2^2\}/(\zeta_1^2+\zeta_2^2)$$
$$\zeta_4=2\zeta_2/(\zeta_1^2+\zeta_2^2)$$
$$\rho_{1x}=\frac{2\sqrt{\zeta}\,\rho_xw_t(0)/w_1\cdot\exp(jgl_1)}{1-\zeta\exp(2jgl_1)}$$
$$\cdot[(\zeta_1+j\zeta_2)(\zeta_1-2+j\zeta_2)]^{-1/2}$$
$$\rho_{1y}=\frac{\sqrt{2\zeta}\,\rho_yw_t(0)/w_1\cdot\exp(jgl_1)}{1-\zeta\exp(2jgl_1)}$$
$$\cdot[(\zeta_1+j\zeta_2)(\zeta_1-2+j\zeta_2)]^{-1/2}. \tag{23}$$

The transmitted Gaussian beam F^t contains unknown quantities of w_2 and z_2. In general, the unknown quantities of w_2 and z_2 can be obtained by maximizing the fundamental mode expansion coefficient absolute value $|t_{00}|$, that is

$$\frac{\partial|t_{00}|}{\partial w_2}=0$$
$$\frac{\partial|t_{00}|}{\partial z_2}=0 \tag{24}$$

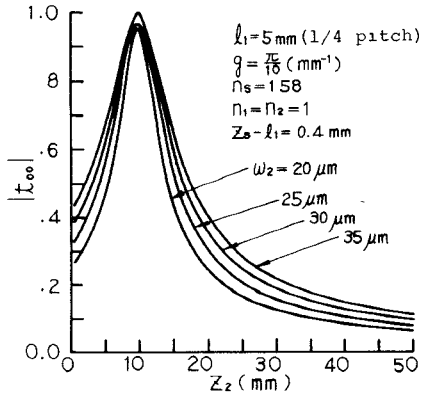

Fig 4 Absolute value $|t_{00}|$ of the transmitted expansion coefficient of the fundamental mode versus w_2 and z_2, when the radiated beam from a single-mode fiber is incident on the square law medium without off-axis and tilt.

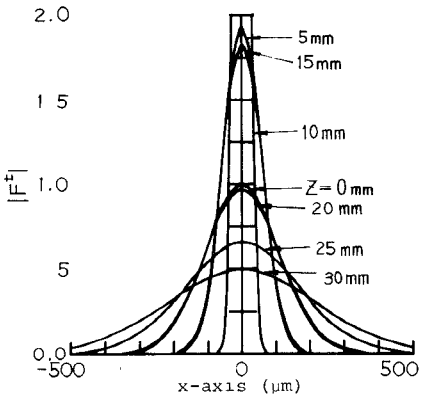

Fig 5. Calculated results of the transmitted Gaussian beam $|F^t|$ under the same conditions as those in Fig 4.

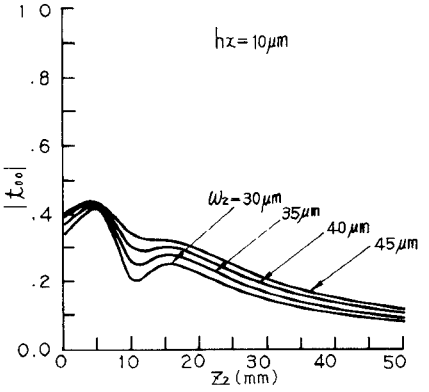

Fig. 6. Absolute value $|t_{00}|$ of the transmitted expansion coefficient of the fundamental mode versus w_2 and z_2, when the radiated beam from a single-mode fiber is incident on the square law medium with a single-mode fiber off-axis quantity of 10 μm.

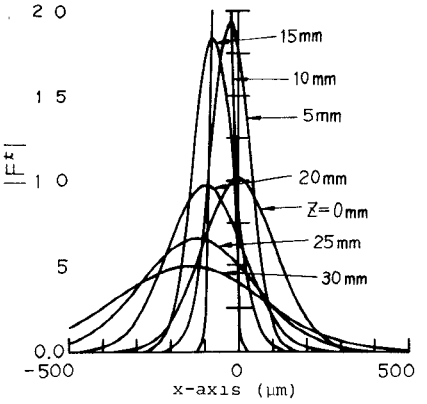

Fig 7. Calculated results of the transmitted Gaussian beam $|F^t|$ under the same conditions as those in Fig. 6.

However, the transmitted Gaussian beam F^t can be obtained, even when w_2 and z_2 have any value, as the transmitted Gaussian beam contains all of the mode. Fig. 4 shows the absolute value $|t_{00}|$ of the transmitted expansion coefficient of the fundamental mode when the radiated beam from a single-mode fiber is incident on the square law medium without being off-axis and tilted. In Fig. 4, it is seen that $|t_{00}|$ is 1 at w_2 ($=30$ μm) and z_2 ($=9.5$ mm), and that only the fundamental mode is excited. Fig. 5 shows the calculated results for the field distribution of the transmitted Gaussian beam $|F^t|$ under the same conditions as those in Fig. 4. In Fig. 5, the field distribution of the transmitted Gaussian beam $|F^t|$ is symmetrical with respect to the z-axis and has a beam waist at about $z=10$ mm and then expands.

Fig. 6 shows the absolute value $|t_{00}|$ of the transmitted expansion coefficient of the fundamental mode, when the radiated beam from a single-mode fiber is incident on the square law medium with a 10-μm off-axis of a single-mode fiber. In Fig. 6, $|t_{00}|$ is only about 0.42 as a maximum value, and the variance in $|t_{00}|$ versus w_2 and z_2 is very complex. Therefore, the transmitted Gaussian beam F^t contains higher modes. Fig. 7 shows the calculated results for the field distribution of the transmitted Gaussian beam $|F^t|$ at the same conditions as those in Fig. 6. In Fig. 7, the transmitted Gaussian beam $|F^t|$ is almost symmetrical with respect to the optical axis of the square law medium on the boundary plane ($z=0$). Accordingly, the center axis of $|F^t|$ expands in the negative direction of the x-axis, as the beam transmits in the z-direction.

IV. Ray Matrix Analysis

The ray matrix analysis of a coupling system between a single-mode fiber and a square law medium was made in order to make clear the relation between the ray matrix analysis and the electromagnetic field analyzed in this paper.

In general, analysis by complex beam parameter Q handles the transformation of beam parameter (such as beam width and plane wavefront curvature) by lens system [11]. Complex beam parameter Q is expressed with spot size w and the radius R of beam curvature by

$$\frac{1}{Q}=\frac{1}{R}-j\frac{\lambda}{\pi w^2}. \tag{25}$$

On the other hand, there is, in general, a linear relation between the input quantities (position x_1 and slope x_1' of the ray in the input plane) and the output quantities (position x_2 and slope x_2' of the ray in the output plane) which can be written in matrix form as

$$\begin{pmatrix} x_2 \\ x_2' \end{pmatrix}=\begin{pmatrix} A & B \\ C & D \end{pmatrix}\begin{pmatrix} x_1 \\ x_1' \end{pmatrix} \tag{26}$$

Complex beam parameter Q_2 in the output plane is given by

$$Q_2 = \frac{AQ_1 + B}{CQ_1 + D} \tag{27}$$

where Q_1 is the complex beam parameter in the input plane. The ray matrix from the output plane ($z = -z_s$) of a single-mode fiber to the position $z = z_{2\gamma}$ of the beam waist in the transmitted Gaussian beam in dielectric #2, as shown in Fig. 8, is given by

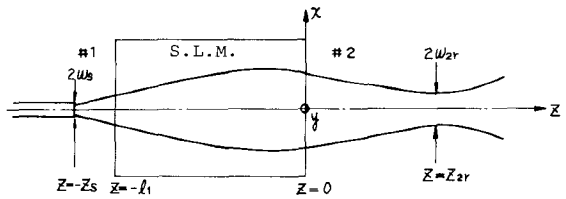

Fig. 8. Radius w_{2r} and position z_{2r} in the beam waist for the transmitted Gaussian beam in dielectric # 2

$$\begin{pmatrix} A & B \\ C & D \end{pmatrix} = \begin{pmatrix} \{\cos(gl_1) - n_s z_{2r} g \sin(gl_1)\} & \left\{((z_s - l_1) + z_{2r})\cos(gl_1) + \left(\frac{1}{n_s g} - n_s g z_{2r}(z_s - l_1)\right)\sin(gl_1)\right\} \\ \{-gn_s \sin(gl_1)\} & \{-n_s g(z_s - l_1)\sin(gl_1) + \cos(gl_1)\} \end{pmatrix}. \tag{28}$$

By substituting (25) into (27),

$$\frac{1}{R_{2r}} - j\frac{\lambda}{\pi w_{2r}^2} = \frac{C - j\left(\frac{\lambda}{\pi w_s^2}\right)D}{A - j\left(\frac{\lambda}{\pi w_s^2}\right)B} \tag{29}$$

where λ is wavelength in dielectrics #1 and #2, $n_1 = n_2 = 1$ and w_{2r} and R_{2r} are the beam waist radius and the radius of curvature in the beam waist for the transmitted Gaussian beam. When R_{2r} in (29) is infinite, that is, the real part of complex number expanded on the right side of (29) is zero, as a result of substituting (28) into (29), then the beam waist position z_{2r} is given by

$$\begin{aligned} z_{2r} = \Bigg[& (\lambda/\pi w_s^2)^2 (z_s - l_1)\cdot\{\sin^2(gl_1) - \cos^2(gl_1)\} \\ & + \left[gn_s + (\lambda/\pi w_s^2)^2 \left\{ n_s g(z_s - l_1)^2 - \frac{1}{n_s g} \right\} \right] \\ & \cdot \cos(gl_1)\sin(gl_1) \Bigg] \\ & / \Big[\left\{ g^2 n_s^2 + (\lambda/\pi w_s^2)^2 n_s^2 g^2 (z_s - l_1)^2 \right\} \sin^2(gl_1) \\ & + (\lambda/\pi w_s^2)^2 \cos^2(gl_1) - 2(\lambda/\pi w_s^2)^2 \\ & \cdot n_s g(z_s - l_1)\cos(gl_1)\sin(gl_1) \Big]. \end{aligned} \tag{30}$$

As the imaginary parts of both the right and left sides of (29) are equal, radius $w_{2\gamma}$ for the beam waist is given by

$$\begin{aligned} w_{2\gamma} = w_s \Bigg[& \Bigg[\{\cos(gl_1) - n_s z_{2r} g \sin(gl_1)\}^2 + (\lambda/\pi w_s^2)^2 \left[\{(z_s - l_1) + z_{2\gamma}\}\cos(gl_1) + \left\{ \frac{1}{n_s g} - n_s g(z_s - l_1) z_{2\gamma} \right\} \sin(gl_1) \right]^2 \Bigg] \\ & / \Big[\{\cos(gl_1) - n_s g(z_s - l_1)\sin(gl_1)\}\{\cos(gl_1) - n_s z_{2\gamma} g \sin(gl_1)\} \\ & + gn_s \sin(gl_1) \left[\{(z_s - l_1) + z_{2\gamma}\}\cos(gl_1) + \left\{ \frac{1}{n_s g} - n_s g(z_s - l_1) z_{2\gamma} \right\} \sin(gl_1) \right] \Big] \Bigg]^{1/2}. \end{aligned} \tag{31}$$

Therefore, the transmitted beam passed through the square law medium is a Gaussian beam given by

$$\begin{aligned} \psi_{\text{out}}(x, y, z) = & \sqrt{\frac{2}{\pi}} \frac{1}{w_{\text{out}}(z)} \\ & \cdot \exp\{-(x^2 + y^2)/w_{\text{out}}(z)^2\} \\ & \cdot \exp\Big[-j\{k_0 z - \phi_{\text{out}}(z)\} \\ & - j\frac{k_0(x^2 + y^2)}{2R_{\text{out}}(z)} \Big] \end{aligned} \tag{32}$$

and

$$\begin{aligned} w_{\text{out}}(z) &= w_{2\gamma}\left[1 + \left\{2(z - z_{2\gamma})/k_0 w_{2\gamma}^2\right\}^2\right]^{1/2} \\ R_{\text{out}}(z) &= (z - z_{2\gamma})\left[1 + \left\{k_0 w_{2\gamma}^2/2(z - z_{2\gamma})\right\}^2\right] \\ \phi_{\text{out}}(z) &= \tan^{-1}\left\{\frac{2(z - z_{2\gamma})}{k_0 w_{2\gamma}^2}\right\}. \end{aligned} \tag{33}$$

The transmitted Gaussian beam F^t, analyzed by electromagnetic field analysis, is compared with the transmitted Gaussian beam ψ_{out} analyzed by ray matrix analysis. Assuming that the transmitted Gaussian beam in (22) is not

off axis and tilted, (22) is given by

$$F^t(x,y,z)=4\sqrt{\frac{2}{\pi}}\frac{1}{w_{l1}}\frac{w_i(0)}{w_i(z)}(\zeta_7+j\zeta_8)\cdot\exp\left[-\frac{(x^2+y^2)}{w_i(z)^2}\cdot\frac{(1-\zeta_5^2-\zeta_6^2)}{\{(1-\zeta_5)^2+\zeta_6^2\}}\right]\cdot\exp\left[-j\left\{n_2k_0z-\phi_i(z)+\left(\frac{n_2k_0}{2R_i(z)}+\frac{2\zeta_6/w_i(z)^2}{\{(1-\zeta_5)^2+\zeta_6^2\}}\right)\cdot(x^2+y^2)+n_sk_0z_s-gl_1+\phi_i(0)-\tan^{-1}\left\{\frac{2(z_s-l_1)}{n_sk_0w_s^2}\right\}\right\}\right] \tag{34}$$

and

$$A_1=\left\{\left(\frac{w_1}{w_{l1}}\right)^4-1+\left(\frac{n_1k_0w_1^2}{2R_{l1}}\right)^2\right\}/\left\{\left(1+\frac{w_1^2}{w_{l1}^2}\right)^2+\left(\frac{n_1k_0w_1^2}{2R_{l1}}\right)^2\right\}$$

$$A_2=n_1k_0w_1^2/R_{l1}/\left\{\left(1+\frac{w_1^2}{w_{l1}^2}\right)^2+\left(\frac{n_1k_0w_1^2}{2R_{l1}}\right)^2\right\}$$

$$A_3=A_1\cos(2gl_1)-A_2\sin(2gl_1)$$

$$A_4=A_1\sin(2gl_1)+A_2\cos(2gl_1)$$

$$\zeta_1=1+\frac{w_i(0)^2}{w_1^2}(1-A_3^2-A_4^2)/\{(1-A_3)^2+A_4^2\}$$

$$\zeta_2=2\frac{w_i(0)^2}{w_1^2}A_4/\{(1-A_3)^2+A_4^2\}-n_2k_0w_i(0)^2/2R_i(0)$$

$$\zeta_5=\zeta_3\cos2\{\phi_i(z)-\phi_i(0)\}-\zeta_4\sin2\{\phi_i(z)-\phi_i(0)\}$$

$$\zeta_6=\zeta_3\sin2\{\phi_i(z)-\phi_i(0)\}+\zeta_4\cos2\{\phi_i(z)-\phi_i(0)\}$$

$$\zeta_7=\left\{\left(1+\frac{w_1^2}{w_{l1}^2}\right)(1-A_3)+\frac{n_1k_0w_1^2A_4}{2R_{l1}}\right\}(\zeta_1-\zeta_1\zeta_5+\zeta_2\zeta_6)-\left\{A_4\left(1+\frac{w_1^2}{w_{l1}^2}\right)-\frac{n_1k_0w_1^2}{2R_{l1}}(1-A_3)\right\}(\zeta_1\zeta_6-\zeta_2+\zeta_2\zeta_5)$$

$$\zeta_8=\left\{\left(1+\frac{w_1^2}{w_{l1}^2}\right)(1-A_3)+\frac{n_1k_0w_1^2A_4}{2R_{l1}}\right\}(\zeta_1\zeta_6-\zeta_2+\zeta_2\zeta_5)+\left\{A_4\left(1+\frac{w_1^2}{w_{l1}^2}\right)-\frac{n_1k_0w_1^2(1-A_3)}{2R_{l1}}\right\}(\zeta_1-\zeta_1\zeta_5+\zeta_2\zeta_6). \tag{35}$$

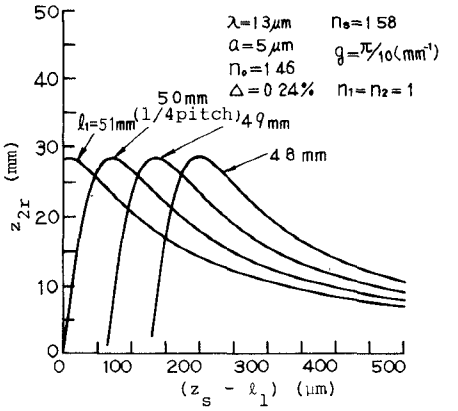

Fig. 9 Ray matrix analysis results of position z_{2r} of the beam waist versus the distance (z_s-l_1) between a fiber and a square law medium as a parameter of the square law medium length l_1.

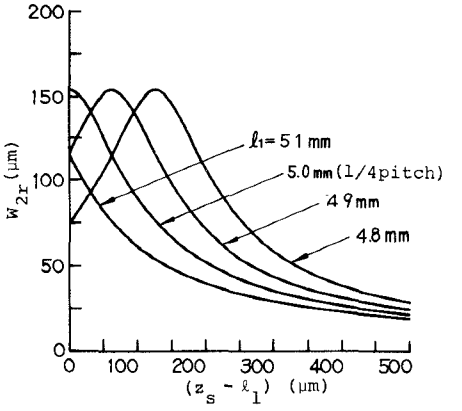

Fig. 10. Ray matrix analysis results of the radius w_{2r} of the beam waist versus the distance (z_s-l_1) between a fiber and a square law medium as a parameter of the square law medium length l_1.

Fig. 9 shows the ray matrix analysis results of position $z_{2\gamma}$ of the beam waist versus the distance (z_s-l_1) between a fiber and a square law medium as a parameter of length l_1 of the square law medium. In Fig. 9, when the square law medium length is 5 mm (1/4 pitch), the position $z_{2\gamma}$ of the beam waist is as far from the square law medium, as the distance (z_s-l_1) between the fiber and the square law medium is large. At a distance (z_s-l_1) of about 75 μm, $z_{2\gamma}$ is the largest value of about 28 mm. Then, the position $z_{2\gamma}$ gradually brings the square law medium closer. In Fig. 9, there is almost no change in the maximum value of $z_{2\gamma}$, even if length l_1 of the square law medium changes. Fig. 10 shows the ray matrix analysis results for radius $w_{2\gamma}$ of the beam waist versus the distance (z_s-l_1) between a fiber and a square law medium as a parameter of length l_1 of the square law medium. In the case where $l_1=5$ mm (1/4 pitch) in Fig. 10, the reason why the beam waist radius $w_{2\gamma}$ is largest at distance $(z_s-l_1)=0$ μm is that the beam waist exists on the boundary plane $(z=0)$ of the square law medium. Fig. 11 shows the ray matrix analysis results for position $z_{2\gamma}$ of the beam waist versus the distance (z_s-l_1) between a fiber and a square law medium as a parameter of the focusing parameter g. As shown in Fig. 11, it is found that, when making the distance between two square

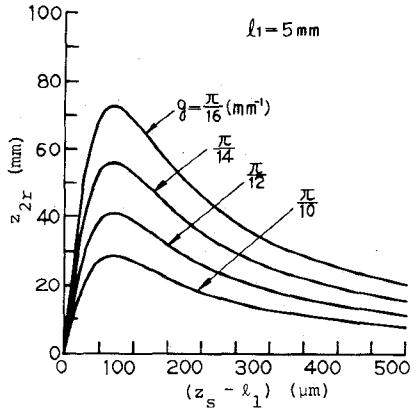

Fig. 11. Ray matrix analysis results of the position z_{2r} of the beam waist versus the distance $(z_s - l_1)$ between a fiber and a square law medium as a parameter of a focusing parameter g.

law media long when designing optical devices, a square law medium is needed with the small focusing parameter g.

The electromagnetic analysis results analyzed in this paper agreed well with the ray matrix analysis results with regard to the analyses in Fig. 9, Fig. 10, and Fig. 11.

V. Coupling Characteristics between Single-Mode Fiber and Square Law Medium

A. Coupling Efficiency Formula

In analyzing the coupling characteristics between the single-mode fiber and square law medium, single-mode fibers and square law media are arranged as shown in Fig. 12. Coupling characteristics are considered between the transmitted Gaussian beam F_0^t of the output beam from fiber 1 and the transmitted Gaussian beam F_i^t of the output beam from fiber 101 at the middle point $z = l_2$ between two square law media. F_0^t and F_i^t are given by (22). Coupling efficiency η derived by electromagnetic field analysis is given by

$$\eta = \frac{\left| \iint_{-\infty}^{\infty} F_0^t(x, y, l_2) F_i^t(x, y, l_2)\, dx\, dy \right|^2}{\iint_{-\infty}^{\infty} |F_0^t(x, y, l_2)|^2\, dx\, dy \iint_{-\infty}^{\infty} |F_i^t(x, y, l_2)|^2\, dx\, dy}. \tag{36}$$

Coupling efficiency η_{ABCD} derived by ray matrix analysis is given by

$$\eta_{ABCD} = \frac{4}{w_o^2(l_2) w_i^2(l_2)} \frac{1}{\{(1/w_o^2(l_2)) + (1/w_i^2(l_2))\}^2 + \{(n_2 k_0 / 2R_o(l_2)) + (n_2 k_0 / 2R_i(l_2))\}^2} \tag{37}$$

where $w_o(l_2)$ and $w_i(l_2)$ are the radii for the spot size of the Gaussian beam transmitted from fiber 1 and fiber 101 at $z = l_2$, respectively, and $R_o(l_2)$ and $R_i(l_2)$ are the radii for the curvature of the wavefront, respectively.

B. Experimental Setup

In order to clarify the theoretical analysis validity, a coupling experiment was made between two single-mode fibers using two square law media. The single-mode fiber used in the experiment was a silica fiber with a 10-μm core diameter, 125-μm fiber diameter, and 0.24-percent relative refractive-index difference between the core and cladding: it was fabricated by the conventional MCVD method. In the coupling experiment, two kinds of square law media were used. One kind has an approximately 0.32 mm^{-1} focusing parameter, 1.58 center refractive index, and 1.8-mm diameter. The other has an approximately 0.09 mm^{-1} focusing parameter, 1.58 center refractive index and 5-mm diameter. Fig. 13 illustrates an aberration testing system for evaluating aberration in the square law medium used in the coupling experiment. A mesh with 2-mm intervals and a 0.6-mm width constant line is employed as the pattern observed through the square law medium sample. The mesh is irradiated by monochromatic light obtained by using a monochromator or color filters. Fig. 14 shows an

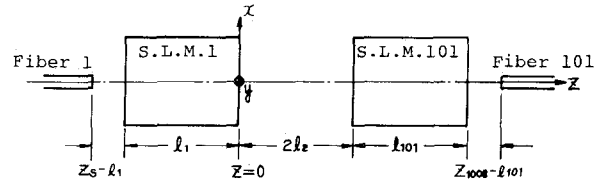

Fig. 12. Coupling system configuration between two single-mode fibers through two square law media.

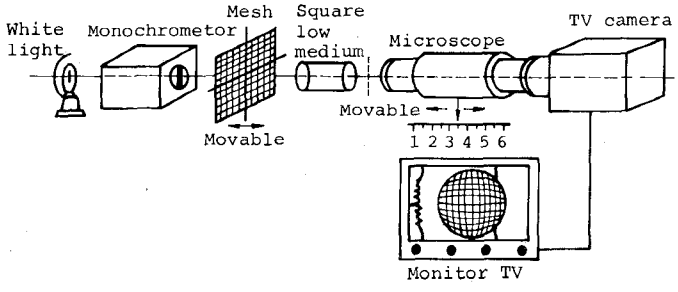

Fig. 13. Testing system for evaluating aberration in the square law medium used in the coupling experiment.

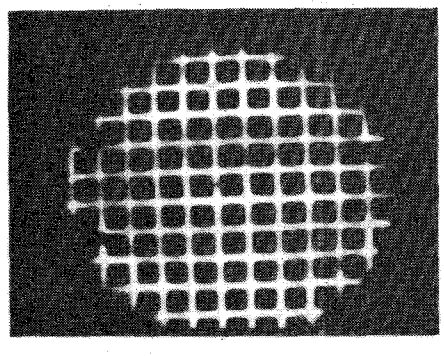

Fig. 14. Image of meshes formed by a square law medium sample, as seen through a microscope with a TV monitor.

TABLE I
SINGLE-MODE FIBER PARAMETERS

Core diameter	10 μm
Fiber diameter	125 μm
Relative refractive-index difference	0.24%
V-number (1.3 μm)	2.44
Calculated spot size	5.4 μm

TABLE II
SQUARE LAW MEDIA PARAMETERS

	Category 1	Category 2
Center refractive index	1.58	1.58
Focusing parameter g	0.32 mm^{-1}	0.09 mm^{-1}
Diameter	1.8 mm	5.0 mm
Length	4.7 mm	16.5 mm

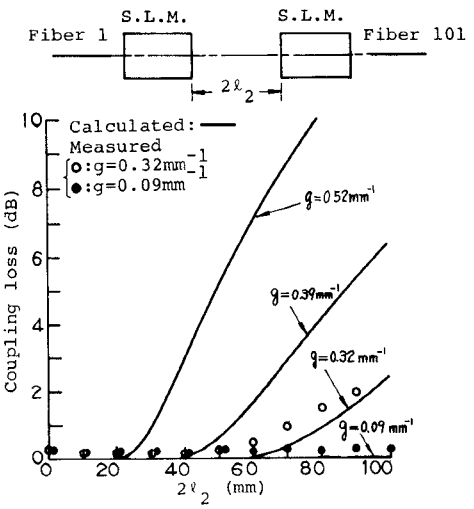

Fig. 15. Results of the theoretical analysis and the experiment on the fiber–fiber coupling loss versus the interval length $2l_2$ between two square law media as a parameter of a focusing parameter g.

image of the mesh which is formed by a square law medium sample as seen through a microscope, with a TV monitor used for screening and precise measurement. As shown in the mesh image in Fig. 14, almost no image distortion is observed at the center of the image, although there is some at the periphery of the image. All the coupling elements (two single-mode fibers and two square law media) were mounted independently on precise manipulators to obtain the maximum coupling efficiency. As a light source, a InGaAsP/InP DH laser diode emitting at a 1.30-μm wavelength was used. Output power was kept constant below 0.1 dB by the use of an automatic power control (APC) circuit. A Ge photodiode with a 2-mm diameter was used to detect both the output power of the input single-mode fiber and the output power of the output single-mode fiber. Tables I and II summarize both the single-mode fiber parameters and square law media parameters used in the coupling experiment, respectively.

C. Optimum Coupling Efficiency

The lens used in optical devices require the following characteristics: 1) low coupling loss; 2) long interval length between two lenses with low coupling loss; 3) large permissible tolerance.

Among them, 1) is the most important for all the optical devices. 2) is especially important for multi/demultiplexers because the multiplexed or demultiplexed light passes through the common glass plate, whose length is 20–100 mm, by bouncing between the optical filters. 3) is necessary in the practical assembly process of the optical devices. The other important characteristics of the lenses are 4) their off-axis and tilt characteristics. In this section, at first, the optimum coupling efficiency is discussed. Fig. 15 shows the results of the electromagnetic field analysis and the experiment on the fiber–fiber coupling loss when the distance $(z_s - l_1)$ between a fiber and a square law medium is chosen so as to minimize the coupling loss versus the interval length $2l_2$ between two square law media as a parameter of the focusing parameter g. In the analysis, calculations are made by using the focusing parameters g, other than those used for the experiment. In the range of the distance $(z_s - l_1)$, which can be chosen so that the interval length $2l_2$ may be twice as long as the interval length $z_{2\gamma}$ between the location of the beam waist of the transmitted Gaussian beam and the output plane of the square law medium, the theoretical coupling loss is 0 dB. At the interval length $2l_2$ above the length twice as long as the interval length $z_{2\gamma}$, the coupling loss rapidly increases. When the focusing parameter g is small, the length $2l_2$, in which the coupling loss is 0 dB, can be long, because the maximum beam waist length is long. In the case of $g = 0.32$ mm^{-1}, the length $2l_2$, in which the coupling loss is 0 dB in the theoretical analysis, is about 60 mm and the length $2l_2$, in which the coupling loss is 0.2–0.3 dB in the experiment, is about 55 mm. In the case of $g = 0.09$ mm^{-1}, the above length $2l_2$ in both the theoretical analysis and the experiment is longer than 100 mm. As mentioned above, the fiber–fiber coupling loss using two square law media is very small. Therefore, the square law media can be applied in many single-mode fiber optical devices. Especially, square law media with 0.09-mm^{-1} focusing parameter can be applied in the multi/demultiplexer because the length $2l_2$ is longer than 100 mm.

D. Off-Axis and Tilt Characteristics

Next, coupling characteristics are considered along with their off-axis and tilt characteristics. The coupling efficiency along with these off-axis and tilt characteristics can be solved using only electromagnetic field analysis. Fig. 16 shows the results of the theoretical analysis and the experiment on the fiber–fiber coupling loss, when only fiber 1 is displaced under the condition of the optimum interval length $2l_2 = 2z_{2\gamma}$ versus the displacement $\Delta x(\Delta y)$ as a parameter of $2l_2$ in the case where $g = 0.09$ mm^{-1}. The coupling loss calculated by theoretical analysis, when

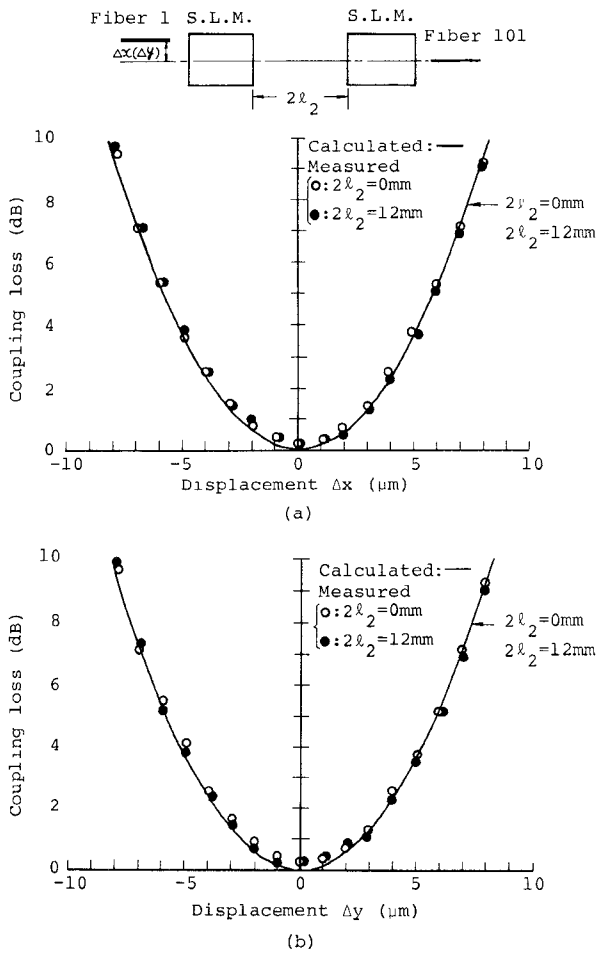

Fig. 16. Results of the theoretical analysis and the experiment on the fiber–fiber coupling loss when only fiber 1 is displaced under the optimum interval length $2l_2 = 2z_{2f}$ state under the same conditions as those in Fig. 15 in the case of $g = 0.09$ mm^{-1}. (a) and (b) represent the results in the x-axis and y-axis, respectively.

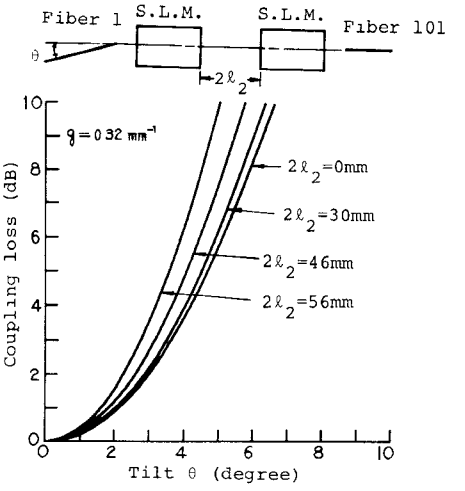

Fig. 17. Theoretical analysis results of the fiber–fiber coupling loss when only fiber 1 is tilted under the same conditions as those in Fig. 15 in the case of $g = 0.32$ mm^{-1}.

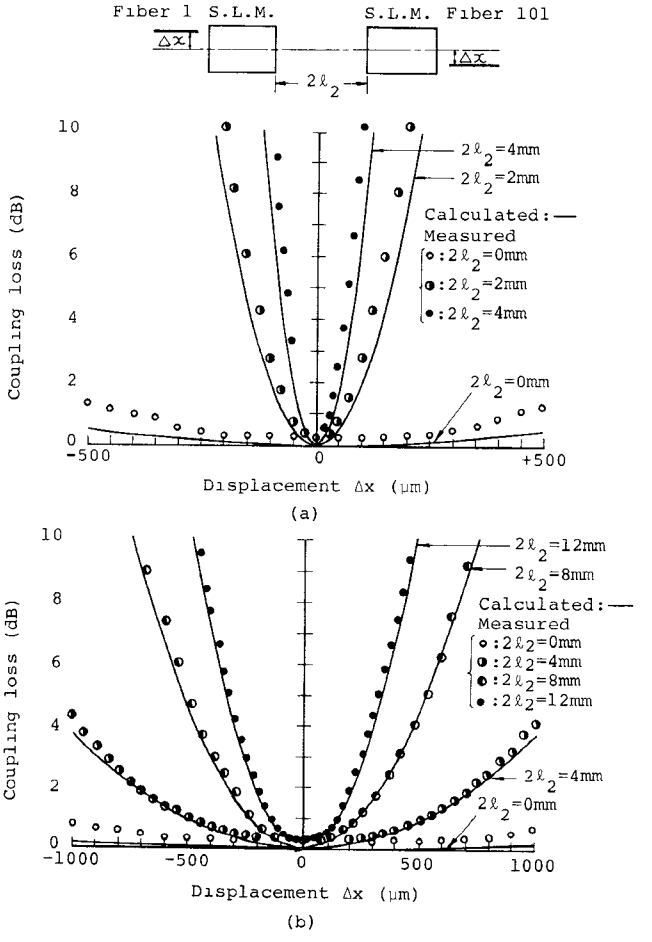

Fig. 18. Results of the theoretical analysis and the experiment on fiber–fiber coupling loss when fiber 1 and fiber 101 are displaced by the same off-axis quantities in the reverse x-direction under the optimum interval length $2l_2 = 2z_{2f}$ condition versus displacement Δx as a parameter of $2l_2$ under the same conditions as those in Fig. 15. (a) and (b) represent the results in the cases where $g = 0.32$ mm^{-1} and $g = 0.09$ mm^{-1}, respectively.

single-mode fiber 1 with a 10-μm core diameter is displaced by 5 μm from the optical axis of the square law medium, is about 3.7 dB when interval lengths $2l_2$ between two square law media are 0 mm and 12 mm. The value of the theoretical analysis almost agrees with the experimental result. The coupling loss versus off-axis quantities is almost unchanged, even when interval length $2l_2$ changes. As a result of the theoretical analysis and the experiment, about ± 2.5-μm accuracy for the fiber arrangement is required in order to be within a coupling loss increase of 1 dB. The results of the theoretical analysis and the experiment for $g = 0.32$ mm^{-1} are the same as those for $g = 0.09$ mm^{-1}. Fig. 17 shows the results of the theoretical analysis on the fiber–fiber coupling loss, when only fiber 1 is tilted under the same conditions as those in Fig. 15 in case of $g = 0.32$ mm^{-1}. As the interval length $2l_2$ is larger, the coupling loss versus the same tilt quantities is larger. This is the reason why the off-axis quantity for the Gaussian beam versus the same tilt quantity are larger, as the distance $(z_s - l_1)$ becomes larger.

E. Off-Axis Tolerance

In the practical assembly process of optical devices such as optical switches and couplers, the permissible tolerance for coupling is as important as the coupling efficiency itself. The influence of the off-axis of the input single-mode fiber is reduced by adjusting the position of the output

single-mode fiber. Accordingly, the coupling-loss increase by a single-mode fiber setting error has been measured by adjusting the output fiber position. Fig. 18 shows the results of the theoretical analysis and the experiment on the fiber–fiber coupling loss, when fibers 1 and 101 are displaced by the same off-axis quantities in the reverse x-direction under the optimum interval length $2l_2 = 2z_{2\gamma}$ state versus the displacement Δx as a parameter of $2l_2$. Fig. 18(a) and (b) shows, the results of both $g = 0.32\ \mathrm{mm}^{-1}$ and $g = 0.09\ \mathrm{mm}^{-1}$, respectively. When the focusing parameter g is small, the length $2l_2$, in which the coupling loss is small when fibers 1 and 101 are displaced with the same off-axis quantities in the reverse x-direction, can be long, as shown in Fig. 18(b). Although the coupling loss in the theoretical analysis almost agrees with that in the experiment in the case of $g = 0.09\ \mathrm{mm}^{-1}$, the coupling loss in the experiment is larger than that in the theoretical analysis in the case of $g = 0.32\ \mathrm{mm}^{-1}$. This is the reason why in the case of $g = 0.32\ \mathrm{mm}^{-1}$ the higher order aberration of the refractive index of the square law medium influences the coupling loss.

VI. Conclusion

The coupling characteristics between a single-mode fiber and a square law medium have been theoretically and experimentally discussed in order to obtain the optimum coupling design for a variety of single-mode fiber optical devices. In theoretically analyzing the coupling efficiency, a Gaussian beam in a dielectric passed through a square law medium has been evaluated with the help of mode-expansion technique and one of the generating functions of the Hermite polynomials. As a result, coupling efficiency has been analytically obtained even when the output beam from a single-mode fiber is off-axis and tilted. Through this analysis, it has been made clear that the ray matrix analysis used previously agrees with the analysis that does not consider the off-axis and tilt factors analyzed in this paper. This analysis may be applied in the development of many single-mode fiber optical devices, such as lens connectors, optical switches, and laser modules. The experimental results concerning the optimum coupling design of the off-axis characteristics and the off-axis tolerances have been presented, and they agree well with the theoretical analysis. As the coupling loss between two single-mode fibers through two square law media is almost 0.2–0.3 dB experimentally in the optimum coupling, the square law media can be applied in many single-mode fiber optical devices.

Acknowledgment

The authors wish to thank K. Fujisaki for his fruitful advice and valuable discussion during this work.

References

[1] K. Nawata, "Multimode and single-mode fiber connectors technology," *IEEE J. Quantum Electron.*, vol. QE-16, pp. 618–627, June 1980.
[2] K. Kobayashi, R. Ishikawa, K. Minemura, and S. Sugimoto, "Microoptic devices for fiber-optic communications," *Fiber Integrated Opt.*, vol. 2, pp. 1–7, 1979.
[3] K. Kobayashi and M. Seki, "Microoptic grating multiplexer and optical isolators for fiber-optic communications," *IEEE J. Quantum Electron.*, vol. QE-16, pp. 11–22, Jan. 1980.
[4] R. Ishikawa, K. Kaede, M. Shikada, K. Kobayashi, and K. Nishizawa, "Characteristics of selfoc lens at 1 μm band," *Tech. Group O.Q.E.*, 78–131, pp. 13–18, 1979, IECE, Japan.
[5] D. Marcuse, "Deformation of fields propagating through gas lenses," *Bell Syst. Tech. J.*, vol. 45, pp. 1345–1368, Oct. 1966.
[6] E. A. J. Marcatili, "Off-axis wave-optic transmission in a lens-like medium with aberration," *Bell Syst. Tech. J.*, vol. 46, pp. 149–166, Jan. 1969.
[7] T. Takenaka and O. Fukumitsu, "Some considerations on an optical microdevice with square law media by wave optics," *Trans. IECE Japan*, vol. J62-C, no. 4, pp. 266–273, Apr. 1979.
[8] T. Kitano, H. Matsumura, M. Furukawa, and I. Kitano, "Measurement of fourth-order aberration in a lens-like medium." *IEEE J. Quantum Electron.*, vol. QE-9, pp. 967–971, Oct. 1973.
[9] K. Tanaka and O. Fukumitsu, "Diffraction of an obliquely incident wave beam by a rectangular aperture," *Tech. Group M.W.*, 73–43, 1973, IECE, Japan.
[10] D. Marcuse, "Loss analysis of single-mode fiber splices," *Bell Syst. Tech. J.*, vol. 56, pp. 703–718, 1977.
[11] H. Kogelnik, "Imaging of optical modes- resonators with internal lenses," *Bell Syst. Tech. J.*, vol. 44, pp. 455–494, Mar. 1965.

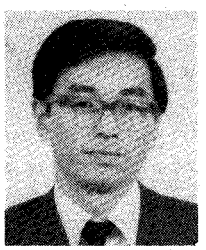

Ryozo Kishimoto was born in Osaka, Japan, on October 19, 1949. He received the B.S. degree in applied physics from Osaka City University, Osaka, Japan, in 1973, and M.S. degree in applied physics from Osaka University, Osaka, Japan, in 1975, respectively.

In 1975 he joined the Yokosuka Electrical Communication Laboratory, Nippon Telegraph and Telephone Public Corporation, Kanagawa, Japan, and he was engaged in research on hydrodynamics for submarine cable. He is now working on optical devices.

Mr. Kishimoto is a Member of the Institute of Electronics and Communication Engineers of Japan and the Japan Society of Mechanical Engineers.

Masaki Koyama (S'64–M'73) was born in Tokyo, Japan, on June 19, 1941. He graduated from Osaka University, Faculty of Engineering, Telecommunication Department, in 1964 and received the Ph.D. degree in 1969 from the same university.

Since joining the Nippon Telegraph and Telephone Electrical Communication Laboratories in 1969, he worked on microwave and millimeter-wave filters for satellite and guided-millimeter-wave transmission systems. After one year stay at ITS/OT, Boulder, CO, from 1972 to 1973, he started research on optical fiber transmission systems and conducted the first overall in-house test of the optical system in 1976. After a period of working at the R&D Bureau from 1978 to 1979 and at the Submarine Communication Section from 1980 to 1981, he moved to the Optical Transmission Section of Yokosuka ECL as a Chief. He now supervises the research and development of optical transmission systems at the above section.

Dr. Koyama is a Member and Technical Referee of the IECE.